

Impact of land use change on soil structure complexity: A horizontal visibility graph analysis using x-ray Computed Tomography (CT)

Impacto da mudança no uso da terra na complexidade da estrutura do solo: Uma análise com grafo de visibilidade horizontal usando tomografia computadorizada de raios-X

Impacto del cambio en el uso de la tierra sobre la complejidad de la estructura del suelo: Un análisis con grafo de visibilidad horizontal mediante tomografía computarizada de rayos X

Received: 02/03/2026 | Revised: 02/11/2026 | Accepted: 02/12/2026 | Published: 02/13/2026

Nicéias Silva Vilela

ORCID: <https://orcid.org/0009-0001-5988-0765>
Federal Rural University of Pernambuco, Brazil
E-mail: niceias.svilela@gmail.com

José Domingos Albuquerque Aguiar

ORCID: <https://orcid.org/0000-0002-9029-7068>
Federal Institute of Education, Science and Technology of Pernambuco, Brazil
E-mail: aguiar.domingos@gmail.com

Tatijana Stosic

ORCID: <https://orcid.org/0000-0002-5691-945X>
Federal Rural University of Pernambuco, Brazil
E-mail: tatijana.stosic@ufrpe.br

Rômulo Simões Cezar Menezes

ORCID: <https://orcid.org/0000-0001-8740-366X>
Federal University of Pernambuco, Brazil
E-mail: rmenezes@ufpe.br

Antonio Celso Dantas Antonino

ORCID: <https://orcid.org/0000-0002-4120-9404>
Federal University of Pernambuco, Brazil
E-mail: acda@ufpe.br

Borko Stosic

ORCID: <https://orcid.org/0000-0001-5031-6968>
Federal Rural University of Pernambuco, Brazil
E-mail: borko.stosic@ufrpe.br

Abstract

The impact of sugarcane management practices on the three-dimensional architecture of soil morphology was quantitatively assessed using complex network analysis of soil images obtained through X-ray computed tomography (CT). This study aims to examine the impact of land-use changes on soil structure by applying the Horizontal Visibility Graph (HVG) method to 3D X-ray computed tomography images of soil samples from the Atlantic Forest and a sugarcane plantation. The HVG method proved effective in characterizing structural changes in the soil samples. Topological indices Clustering Coefficient, Average Shortest Path Length, and Average Degree of the HVG networks, were calculated and found to be correlated with key phenomenological aspects of soil. Among these, the Average Shortest Path Length emerged as the most suitable indicator for quantifying the degradation of soil morphological properties associated with vegetation cover change. Specifically, the transition from Atlantic Forest to sugarcane was shown to alter soil morphology toward greater homogeneity. Overall, these findings demonstrate a clear relationship between the complexity of 3D soil image HVG networks and soil physical properties, highlighting the potential of this approach to quantify soil morphological degradation resulting from land cover change.

Keywords: Horizontal visibility graph; Soil; X-ray computed tomography.

Resumo

O impacto das práticas de manejo da cana-de-açúcar na arquitetura tridimensional da morfologia do solo foi avaliado quantitativamente por meio da análise de redes complexas de imagens de solo obtidas por tomografia computadorizada (CT) de raios-X. Este estudo visa examinar o impacto das mudanças no uso da terra sobre a estrutura do solo, aplicando o método Horizontal Visibility Graph (HVG) a imagens de tomografia computadorizada de raios-X em 3D de amostras de solo da Mata Atlântica e de uma plantação de cana-de-açúcar. O método HVG mostrou-se eficaz na caracterização das mudanças estruturais nas amostras de solo. Os índices topológicos, incluindo

o Coeficiente de Agrupamento, o Comprimento Médio do Caminho Mais Curto e o Grau Médio das redes HVG, foram calculados e demonstraram correlação com aspectos fenomenológicos do solo. Entre eles, o Comprimento Médio do Caminho Mais Curto destacou-se como o indicador mais adequado para quantificar a degradação das propriedades morfológicas do solo associada à mudança da cobertura vegetal. Especificamente, a transição da Mata Atlântica para a cana-de-açúcar mostrou alterações na morfologia do solo em direção a uma maior homogeneidade. De modo geral, esses resultados demonstram uma relação clara entre a complexidade das redes HVG de imagens 3D do solo e suas propriedades físicas, evidenciando o potencial dessa abordagem para quantificar a degradação das propriedades morfológicas de solo decorrente da mudança no uso da terra.

Palavras-chave: Grafo de visibilidade horizontal; Solo; Tomografia computadorizada por raios-X.

Resumen

El impacto de las prácticas de manejo de la caña de azúcar en la arquitectura tridimensional de la morfología del suelo fue evaluado cuantitativamente mediante el análisis de redes complejas de imágenes de suelo obtenidas por tomografía computarizada (CT) de rayos X. Este estudio tiene como objetivo examinar el impacto de los cambios de uso del suelo en la estructura del suelo mediante la aplicación del método de Gráficos de Visibilidad Horizontal (HVG) a imágenes de tomografía computarizada de rayos X 3D de muestras de suelo de la Mata Atlántica y una plantación de caña de azúcar. El método HVG resultó eficaz para caracterizar los cambios estructurales en las muestras de suelo. Los índices topológicos, Coeficiente de Agrupamiento, la Longitud Media del Camino Más Corto y el Grado Medio de las redes HVG, fueron calculados y demostraron correlación con aspectos fenomenológicos del suelo. Entre ellos, la Longitud Media del Camino Más Corto se destacó como el indicador más adecuado para cuantificar la degradación de las propiedades morfológicas del suelo asociada al cambio de cobertura vegetal. En particular, la transición del Bosque Atlántico a la caña de azúcar mostró alterar la morfología del suelo en dirección a una mayor homogeneidad. En general, estos resultados demuestran una relación clara entre la complejidad de las redes HVG de imágenes 3D del suelo y sus propiedades físicas, evidenciando el potencial de este enfoque para cuantificar la degradación de las propiedades morfológicas del suelo derivada del cambio en el uso de la tierra.

Palabras clave: Grafo de visibilidad horizontal; Suelo; Tomografía computarizada de rayos X.

1. Introduction

Soil structure is fundamental to sustainable food production and overall societal well-being. However, economic-driven land-use changes are leading to soil degradation, posing a significant threat to the future in many regions across the globe. Land-use change can negatively impact crucial soil functions, including nutrient storage and recycling, carbon sequestration and greenhouse gas emissions, disease and pest regulation, erosion resistance, water retention, drainage, and filtration (Bordonal et al., 2018; Bünemann et al., 2018; Creamer et al., 2022; Williams, Colombi & Keller, 2020). In response to economic demands and rapid population growth, developing countries are increasingly utilizing natural resources. As forests are cleared for pasture, timber, firewood, and agricultural expansion, vast tropical regions are being converted into farmland at an alarming rate. Therefore, a comprehensive assessment of soil properties is essential to detect early signs of degradation and mitigate its adverse effects.

Research on the impacts of land-use changes has primarily focused on the physical, chemical, and biological properties of soil (Aon et al., 2001; Das et al., 2018; Ozores-Hampton, Stansly & Salame, 2011; Usharani, Roopashree & Naik, 2019), while fewer studies have examined the effects of these changes on soil structure (Aguiar et al., 2023; Soto-Gomez et al., 2020). Soil structure plays a crucial role in regulating its functions, which description and quantification requires a deep understanding of characteristics such as the three-dimensional distribution of components, their connectivity, hierarchical organization, and complexity.

Recent advancements in techniques for assessing soil functions, such as X-ray computed tomography (CT), an efficient and non-destructive method (Soto-Gomez et al., 2020), enabled direct observation of soil structure and its morphological characteristics (Ojeda-Magaña et al., 2014). CT has become a widely used tool for 3D visualization and quantification of soil structure, offering new insights into soil functions (Helliwell et al., 2013). Properties that were once difficult to analyze can now be assessed through CT scans, providing new knowledge on soil structure (Helliwell et al., 2013). These properties include isotropy, homogeneity, complexity, and the hierarchical fractal (or multifractal) organization of soil

constituents, contributing to a deeper understanding of the physical, chemical, and biological processes within soil (Schlüter et al., 2018).

The destruction and degradation of natural ecosystems are among the primary causes of global biodiversity loss (Haddad et al., 2015). Brazil stands out as one of the most significant countries in terms of preserved ecosystems and genetic wealth, hosting approximately 20% of the world's biodiversity. However, between 2000 and 2018, the country experienced a reduction of 489.77 km² in natural areas across its six biomes, representing an 8.3% decline in natural landscapes nationwide. Among these, the Atlantic Forest has suffered the highest percentage of degradation over time, largely due to its concentration of industrial and agricultural activities, as well as the highest population density in the country—encompassing around 49.3% of Brazil's urban areas (IBGE, 2020).

The conversion of native Atlantic Forest vegetation into sugarcane plantations has significantly altered the physical properties of the soil (Bordonal et al., 2018; Cherubin et al., 2015; Franco et al., 2016; Haghghi et al., 2010), which play a crucial role in essential functions such as water retention and absorption, gas exchange, erosion prevention, nutrient cycling, and root development (Rabot et al., 2018), directly impacting ecosystem services.

This study examines the impact of land-use changes on soil structure by applying the Horizontal Visibility Graph (HVG) method to 3D X-ray computed tomography images of soil samples from the Atlantic Forest and a sugarcane plantation. Originally introduced by Luque et al. (2009), HVG is a technique that represents time series as complex networks, allowing for the extraction of topological measures that reveal underlying temporal patterns.

2. Methodology

A mixed research methodology was carried out, partly field research, partly laboratory research, and in a study of a quantitative and qualitative nature (Risemberg, Wakin & Shitsuka, 2026; Pereira et al., 2018) and using descriptive statistics (Vieira, 2021).

2.1 Data

In this study, soil samples were collected from a sugarcane field and a nearby area of native Atlantic Forest in Pernambuco, northeastern Brazil. Samples were obtained using a soil auger equipped with an internal PVC cylinder measuring 7.5 cm in height and 7.5 cm in diameter. To remove excess moisture, the samples were dried at 40°C before undergoing computed tomography (CT) scanning.

Computed tomography was performed using a third-generation Nikon XT H 225 ST X-ray microtomography equipment, operating at a voltage of 150 kV, current of 180 μ A, exposure time of 500 ms, and resolution of 45 μ m for voxels. A copper filter with a thickness of 0.5 mm was used to reduce low-intensity photons. After scanning the total volume of the cylinder in the initial phase of the acquisition, a subvolume of interest was delimited and recreated using the CTPro 3D XT 3.0.3 software (Nikon Metrology NV). The central part of the cylinder was emphasized to avoid interference from the edges.

The axial 2D reconstructions retained the original 45 μ m spatial resolution and were stored in a 16-bit grayscale format. The final dataset comprised 790 stacks of 790 \times 790 pixels, resulting in a total volume of 493,039,000 voxels. The voxel values in the CT images correspond to the local density of the sample. The sequence of voxel values along the vertical axis (aligned with gravity) was considered the most appropriate from a phenomenological standpoint and was interpreted as one-dimensional data analogous to a time series.

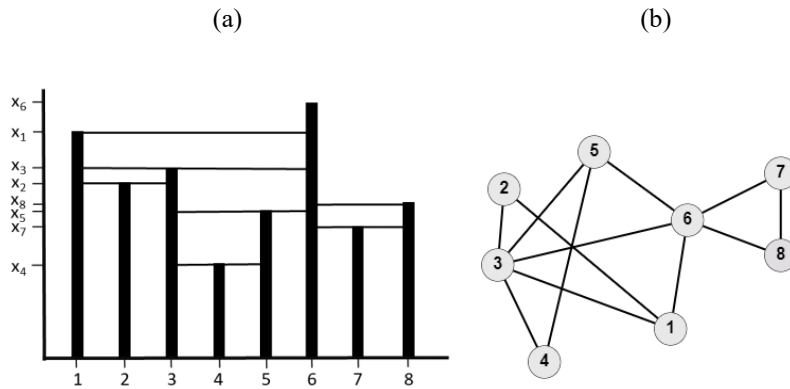
2.2 Horizontal Visibility graph (HVG)

Horizontal visibility graph was introduced by Luque et al (2009) as a method that transforms time series into a network which nodes are data points. Two nodes i and j are connected if a horizontal line can be drawn linking and without intersecting the height (value) of any intermediate data points (Figure 1). Thus, nodes i and j are connected if they satisfy the following geometric criterion of horizontal visibility:

$$x_i, x_j > x_n, \forall n \forall i < n < j$$

HVG is a connected network (every pair of neighbor nodes is connected), and it is invariant under affine transformation (the rescaling and translation of horizontal and vertical axes).

Figure 1: Illustrative example of a time series indicated by vertical bars (a) and its corresponding visibility graph generated by the HVG algorithm (b).



Source: Adapted from Luque et al. (2009).

In this work we calculate the following topological measures of HVG network:

- i) The first measure is the average degree. In a graph, the different nodes may present variations in the number of connections, and this quantity is denominated node degree (k_i). Average degree is the average value of degrees of all nodes in the network:

$$\langle k \rangle = \frac{1}{N} \sum_{i=1}^N k_i$$

- ii) The second measure is global clustering coefficient which represents the average value of local clustering coefficients of all nodes. The local clustering coefficient of node i is calculated as

$$C_i = \frac{E_i}{k_i(k_i - 1)/2}$$

where k_i is the number of nodes connected to node i , E_i is the number of links between these nodes, and $k_i(k_i - 1)/2$ is the maximum number of links between k_i nodes. The values of C_i are between 0 and 1, where $C_i = 0$ is obtained if there are no links between any of k_i nodes that are connected to node i , and $C_i = 1$ is obtained when all k_i nodes are connected. For HVG with N nodes, the global clustering coefficient is defined as

$$C = \frac{1}{N} \sum_{i=1}^N C_i$$

with $0 \leq C \leq 1$. Higher values of C indicate more connected network.

iii) The third measure is the average shortest path length which quantifies the efficiency of information transport between nodes. It is defined as the average number of steps along the shortest paths for all possible pairs of nodes:

$$\langle d_{ij} \rangle = \frac{1}{N(N-1)} \sum_{i,j; i \neq j} d_{ij}$$

where d_{ij} is the shortest path (number of steps) between nodes i and j . Larger values of $\langle d_{ij} \rangle$ indicate more efficient transport of information along the network.

HVG was used in data analysis from various research fields such as medicine (Wang et al., 2017; Zhang et al., 2024), hydrology (Braga et al., 2016; Beltramone et al., 2025), physics (Acosta-Tripailao et al., 2021), chemical (Du et al., 2026) and finances (Vamvakaris et al., 2018, Wei & Xie, 2025).

3. Results and Discussion

In this analysis, the dataset consists of 790×790 one-dimensional vertical lines, each containing 790 grayscale values extracted from X-ray computed tomography images of soil samples collected from a sugarcane field and a nearby site within the Atlantic Forest. For each image and its corresponding HVG-generated network, topological indices were calculated to quantify the structural characteristics of the one-dimensional data.

The topological indices of the HVG network for soil samples from sugarcane field and Atlantic Forest are presented in Table 1 (descriptive statistics), Figure 2 (spatial distribution in the horizontal plane), and Figure 3 (histograms).

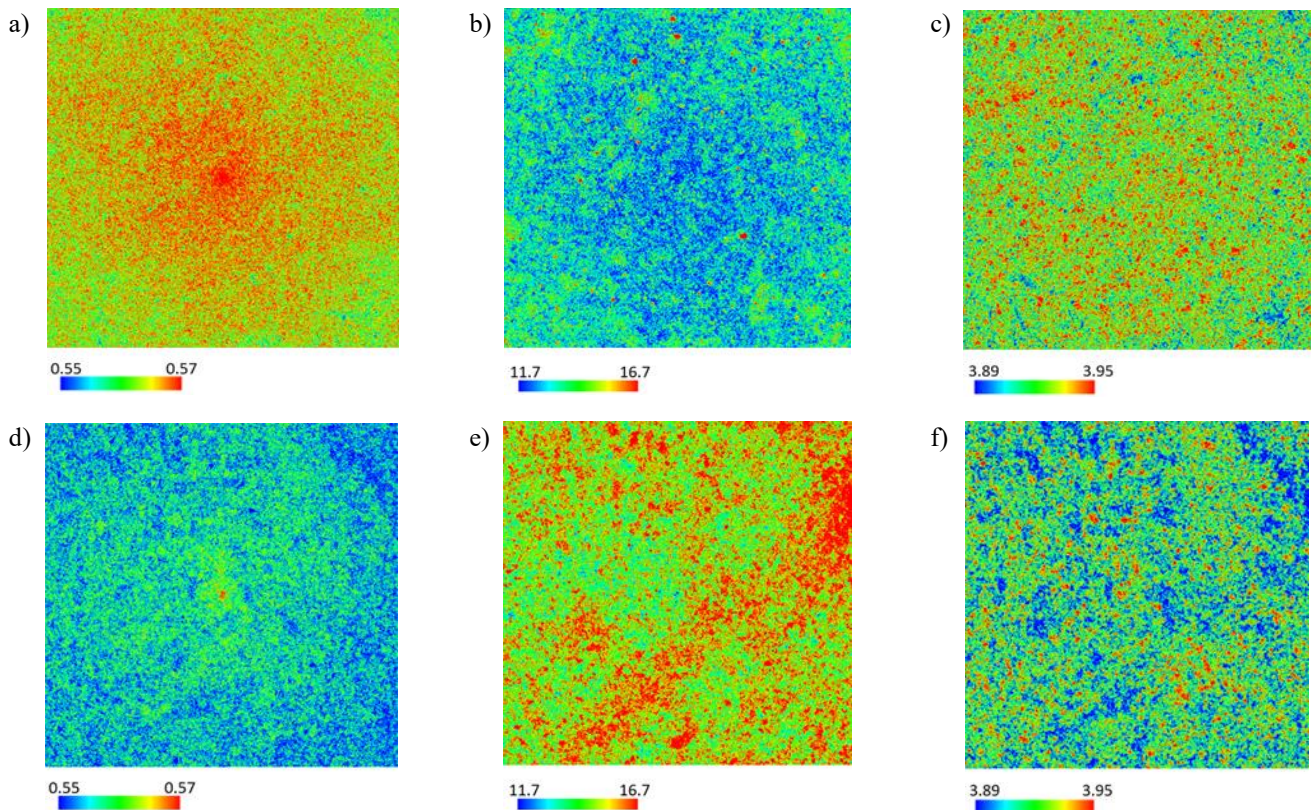
It can be observed in Table 1, that the average shortest path length showed the greatest difference between the two samples. All values are higher for the Atlantic Forest, indicating a network with lower efficiency of information transport. For soil covered by sugarcane, this index decreased, reflecting the fact that the morphological properties of the soil were altered due to the replacement of native vegetation with a sugarcane crop with a repetitive cycle (planting, growth, harvest) and preparation for a new cycle, mainly with the burning of sugarcane residues. This last phase alters the physical, chemical and biological processes of the soil layers near the surface, causing the loss of natural complexity of the soil/vegetation cover system, resulting in a more homogeneous soil structure, generating HVG networks with greater information transmission efficiency (lower average shortest path length). Figure 3 shows overlapping of the histograms of the average degree index and separation of the histograms of the global clustering coefficient and average shortest path length indices. The spatial distribution of the topological indices in the horizontal plane (Figure 2) showed greater heterogeneity for the Atlantic Forest sample than for sugarcane, being more heterogeneous for the average shortest path length. These results indicate that in the HVG analysis the average shortest path length index is most suitable for quantifying the level of soil degradation caused by changes in vegetation cover.

Table 1: Descriptive statistics of the topological indices of the HVG network, calculated for the soil samples collected from sugarcane field (SC) and Atlantic Forest (AF).

| Descriptive statistics | Topological indexes | | | | | |
|------------------------|----------------------------|--------|--|---------|------------------------------------|--------|
| | Clustering coefficient C | | Average shortest path $\langle d_{ij} \rangle$ | | Average degree $\langle k \rangle$ | |
| | SC | AF | SC | AF | SC | AF |
| Mean | 0.5619 | 0.5516 | 13.0848 | 15.3479 | 3.9270 | 3.9163 |
| Standard deviation | 0.0047 | 0.0050 | 1.0976 | 1.3828 | 0.0155 | 0.0184 |
| Minimum | 0.5351 | 0.5235 | 9.4718 | 10.4707 | 3.8253 | 3.8177 |
| 1° Quartile | 0.5588 | 0.5483 | 12.3111 | 14.3717 | 3.9165 | 3.9038 |
| Median | 0.5621 | 0.5518 | 12.9800 | 15.2292 | 3.9266 | 3.9165 |
| 3° Quartile | 0.5651 | 0.5551 | 13.7425 | 16.1920 | 3.9367 | 3.9291 |
| Maximum | 0.5838 | 0.5772 | 21.1245 | 25.1635 | 3.9873 | 3.9848 |

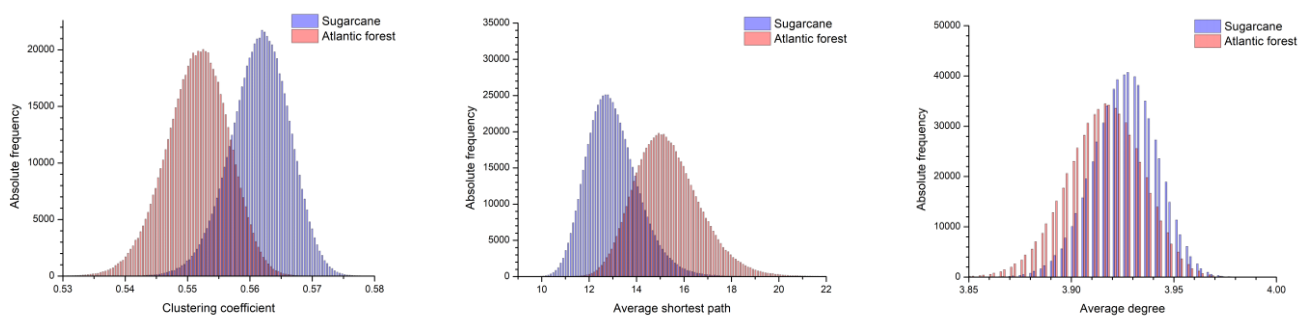
Source: Research data (2026).

Figure 2: Color-coded HVG indices values of the soil sample from sugarcane field, (a) clustering coefficient, (b) average shortest path length, and (c) average degree; and from Atlantic Forest, (d) clustering coefficient (e) average shortest path length and (f) average degree.



Source: Research data (2026).

Figure 3: Histograms of the HVG indices values for the two samples.



Source: Research data (2026).

4. Conclusion

This study proposes the use of the Horizontal Visibility Graph (HVG) method to analyze one-dimensional data derived from computed tomography (CT) images of soils under sugarcane and Atlantic Forest cover. Application of the HVG method to vertical lines of CT images led to the following conclusions:

1. The conversion of vegetation cover from native forest to sugarcane altered the morphological properties of the soil, driving them toward greater homogeneity, increased connectivity, and enhanced efficiency in information transport within HVG networks.
2. The Average Shortest Path Length proved to be the most effective index for distinguishing between the studied samples. It provided a clear quantification of soil morphological degradation associated with vegetation cover change, thereby contributing directly to the development and validation of theoretical and computational models of soil structure.
3. The HVG method, applied here for the first time to three-dimensional soil images, demonstrated efficiency in capturing the structural properties of networks generated from vertical lines of CT data.

As future work, additional topological measures of visibility graphs could be explored to further investigate soil structural behavior. Moreover, variations of the Visibility Graph method may be applied, including the Limited Penetrable Horizontal Visibility Graph (Wang et al., 2017; Jiang et al., 2025), the Weighted Visibility Graph (Azizi & Sulaimany, 2024), and the Multiscale Visibility Graph (Li & Zhao, 2018).

Acknowledgments

The authors acknowledge support from the Brazilian agency FACEPE (grants: APQ-0498-3.07/17 INCT 2014, APQ-0500-5.01/22; CNPq 406202/2022-2). T.S. and B.S. acknowledge support from Brazilian agency CNPq (grants No 308782/2022-4 and 309499/2022-4). B.S. acknowledges support of Brazilian agency CAPES through grant No 88887.937789/2024-00.

References

- Acosta-Tripailao, B., Pastén, D., & Moya, P. S. (2021). Applying the horizontal visibility graph method to study irreversibility of electromagnetic turbulence in non-thermal plasmas. *Entropy*, 23(4), 470. <https://doi.org/10.3390/e23040470>.
- Aon, M. A., Sarena, D. E., Burgos, J. L., & Cortassa, S. (2001). (Micro) biological, chemical and physical properties of soils subjected to conventional or no-till management: An assessment of their quality status. *Soil and Tillage Research*, 60(3–4), 173–186. [https://doi.org/10.1016/S0167-1987\(01\)00190-8](https://doi.org/10.1016/S0167-1987(01)00190-8).

- Aguiar, D., Menezes, R. S. C., Antonino, A. C. D., Stosic, T., Tarquis, A. M., & Stosic, B. (2023). Quantifying soil complexity using Fisher Shannon method on 3D X-ray computed tomography scans. *Entropy*, 25(10), 1465. <https://doi.org/10.3390/e25101465>.
- Azizi, H., & Sulaimany, S. (2024). A review of visibility graph analysis. *IEEE Access*. <https://doi.org/10.1109/ACCESS.2024.3401485>.
- Beltramone, G., Frery, A. C., Scavuzzo, M., & Ferral, A. (2025, August). Snow Phase Change Detection In C-Band Sar Time Series Using Horizontal Visibility Graphs. In IGARSS 2025-2025 *IEEE International Geoscience and Remote Sensing Symposium*, <https://doi.org/10.1109/IGARSS55030.2025.11243921>.
- Bordonal, R. D. O., Carvalho, J. L. N., Lal, R., De Figueiredo, E. B., De Oliveira, B. G., & La Scala, N. (2018). Sustainability of sugar cane production in Brazil. *A review. Agronomy for Sustainable Development*, 38, 1–23. <https://doi.org/10.1007/s13593-018-0490-x>.
- Braga, A. C., Alves, L. G. A., Costa, L. S., Ribeiro, A. A., De Jesus, M. M. A., Tateishi, A. A., & Ribeiro, H. V. (2016). Characterization of river flow fluctuations via horizontal visibility graphs. *Physica A: Statistical Mechanics and its Applications*, 444, 1003–1011. <https://doi.org/10.1016/j.physa.2015.10.102>.
- Bünemann, E. K., Bongiorno, G., Bai, Z., Creamer, R. E., De Deyn, G., De Goede, R., Fleskens, L., Geissen, V., Kuyper, T. W., Mader, P., Pulleman, M., Sukkel, W., Van Groenigen, J. W., Brussaard, L. (2018). *Soil quality—A critical review. Soil Biology and Biochemistry*, 120, 105–125. <https://doi.org/10.1016/j.soilbio.2018.01.030>.
- Cherubin, M. R., Franco, A. L. C., Cerri, C. E. P., da Silva Oliveira, D. M., Davies, C. A., & Cerri, C. C. (2015). Sugar cane expansion in Brazilian tropical soils—Effects of land use change on soil chemical attributes. *Agriculture, Ecosystems & Environment*, 211, 173–184. <https://doi.org/10.1016/j.agee.2015.06.006>.
- Creamer, R. E., Barel, J. M., Bongiorno, G., & Zwetsloot, M. J. (2022). The life of soils: Integrating the who and how of multifunctionality. *Soil Biology and Biochemistry*, 166, 108561. <https://doi.org/10.1016/j.soilbio.2022.108561>.
- Das, A., Lyngdoh, D., Ghosh, P. K., Lal, R., Layek, J., & Idapuganti, R. G. (2018). Tillage and cropping sequence effect on physico-chemical and biological properties of soil in Eastern Himalayas, India. *Soil and Tillage Research*, 180, 182–193. <https://doi.org/10.1016/j.still.2018.03.005>.
- Du, L., Cheng, H., Li, S., Liu, Z., Yang, C., & Du, Y. (2026). Horizontal Visibility Graph Analysis for Flow Regime Recognition in a Gas–Solid Fluidized Bed. *Industrial & Engineering Chemistry Research*, 65, 4, 2274–2287. <https://doi.org/10.1021/acs.iecr.5c04796>.
- Franco, A. L., Bartz, M. L., Cherubin, M. R., Baretta, D., Cerri, C. E., Feigl, B. J., Wall, D. H., Davies, C. A., Cerri, C. C. (2016). Loss of soil (macro) fauna due to the expansion of Brazilian Sugar cane acreage. *Science of the Total Environment*, 563, 160–168. <https://doi.org/10.1016/j.scitotenv.2016.04.116>.
- Haddad, N. M., Brudvig, L. A., Clobert, J., Davies, K. F., Gonzalez, A., Holt, R. D., Lovejoy, T. E., Sexton, J. O., Austin, M. P., Collins, C.D., Cook, W. M., Damschen, E. I., Ewers, R. M., Foster, B. L., Jenkins, C. N., King, A. J., Laurance, W. F., Levey, D. J., Margules, C.R., ... (2015). Habitat fragmentation and its lasting impact on Earth’s ecosystems. *Science Advances*, 1, 2, e1500052. <https://doi.org/10.1126/sciadv.1500052>.
- Haghighi, F., Gorji, M., & Shorafa, M. (2010). A study of the effects of land use changes on soil physical properties and organic matter. *Land Degradation & Development*, 21, 5, 496–502. <https://doi.org/10.1002/ldr.999>.
- Helliwell, J. R., Sturrock, C. J., Grayling, K. M., Tracy, S. R., Flavel, R. J., Young, I. M., Whalley, W. R., Mooney, S.J. (2013). Applications of X-ray computed tomography for examining biophysical interactions and structural development in soil systems: *A review. European Journal of Soil Science*, 64(3), 279–297. <https://doi.org/10.1111/ejss.12028>.
- IBGE, Coordenação de Recursos Naturais e Estudos Ambientais, Coordenação de Contas Nacionais. (2020). Contas de ecossistemas: o uso da terra nos biomas brasileiros: 2000-2018. *Instituto Brasileiro de Geografia e Estatística*, Rio de Janeiro, 73(1), 106.
- Jiang, Y., Hu, J., Chen, X., & Mo, W. (2025). Predicting gas flow rates of wellhead chokes based on a cascade forwards neural network with a historically limited penetrable visibility graph. *Applied Intelligence*, 55, 6, 1–17. <https://doi.org/10.1007/s10489-025-06365-w>.
- Li, W., & Zhao, X. (2018). Multiscale horizontal-visibility-graph correlation analysis of stock time series. *Europhysics Letters*, 122, 4, 40007. [10.1209/0295-5075/122/40007](https://doi.org/10.1209/0295-5075/122/40007).
- Luque, B., Lacasa, L., Ballesteros, F., & Luque, J. (2009). Horizontal visibility graphs: Exact results for random time series. *Physical Review E*, 80, 4, 046103. <https://doi.org/10.1103/PhysRevE.80.046103>.
- Ojeda-Magaña, B., Quintanilla-Domínguez, J., Ruelas, R., Tarquis, A. M., Gómez-Barba, L., & Andina, D. (2014). Identification of pore spaces in 3D CT soil images using PFCM partitional clustering. *Geoderma*, 217, 90–101. <https://doi.org/10.1016/j.geoderma.2013.11.005>.
- Ozores-Hampton, M., Stansly, P. A., & Salame, T. P. (2011). Soil chemical, physical, and biological properties of a sandy soil subjected to long-term organic amendments. *Journal of Sustainable Agriculture*, 35(3), 243–259. <https://doi.org/10.1080/10440046.2011.554289>.
- Pereira, A. S. et al. (2018). Metodologia da pesquisa científica. [free ebook]. Santa Maria: Editora da UFSM.
- Rabot, E., Wiesmeier, M., Schlüter, S., & Vogel, H. J. (2018). Soil structure as an indicator of soil functions: *A review. Geoderma*, 314, 122–137. <https://doi.org/10.1016/j.geoderma.2017.11.009>.
- Risemberg, R. I. C., Wakin, M., & Shitsuka, R. (2026). A importância da metodologia científica no desenvolvimento de artigos científicos. *E-Acadêmica*, 7, 1, e0171675. <https://eacademica.org/eacademica/article/view/675>.
- Schlüter, S., Großmann, C., Diel, J., Wu, G. M., Tischer, S., Deubel, A., & Rücknagel, J. (2018). Long-term effects of conventional and reduced tillage on soil structure, soil ecological and soil hydraulic properties. *Geoderma*, 332, 10–19. <https://doi.org/10.1016/j.geoderma.2018.07.001>.

Soto-Gomez, D., Perez-Rodriguez, P., Juiz, L. V., Paradelo, M., & Lopez-Periago, J. E. (2020). 3D multifractal characterization of computed tomography images of soils under different tillage management: Linking multifractal parameters to physical properties. *Geoderma*, 363, 114129. <https://doi.org/10.1016/j.geoderma.2019.114129>.

Usharani, K. V., Roopashree, K. M., & Naik, D. (2019). Role of soil physical, chemical and biological properties for soil health improvement and sustainable agriculture. *Journal of Pharmacognosy and Phytochemistry*, 8(5), 1256–1267. <https://doi.org/10.22271/phyto>.

Vamvakaris, M. D., Pantelous, A. A., & Zuev, K. M. (2018). Time series analysis of S&P 500 index: A horizontal visibility graph approach. *Physica A: Statistical Mechanics and its Applications*, 497, 41-51. <https://doi.org/10.1016/j.physa.2018.01.010>.

Wang, L., Long, X., Arends, J. B., & Aarts, R. M. (2017). EEG analysis of seizure patterns using visibility graphs for detection of generalized seizures. *Journal of neuroscience methods*, 290, 85-94. <https://doi.org/10.1016/j.jneumeth.2017.07.013>.

Wei, N., & Xie, W. J. (2025). Identifying states of global oil and gas markets based on visibility graph embedding algorithms. *Fluctuation and Noise Letters*, 24, 03, 2550027. <https://doi.org/10.1142/S0219477525500270>.

Williams, H., Colombi, T., & Keller, T. (2020). The influence of soil management on soil health: An on-farm study in southern Sweden. *Geoderma*, 360, 114010. <https://doi.org/10.1016/j.geoderma.2019.114010>.

Zhang, L., Zhou, M., Liu, Y., Xiong, K., Zhang, L., Wu, C., & Lang, H. (2024). Structural Characterization of Horizontal Visibility Network Based on Time Series of Emergency Disease Visits. *Research Square*, 1, 1-15. <https://doi.org/10.21203/rs.3.rs-4436890/v1>.